Thermally Induced Softening of the Radial Breathing Modes of Bundled Single-Walled Carbon Nanotubes

K. P. Meletov[a]; A. V. Krestinin[b]; J. Arvanitidis[cd]; D. Christofilos[c]; G. A. Kourouklis[c]

[a] Institute of Solid State Physics of RAS, Chernogolovka, Moscow Region, Russia [b] Institute of Problems of Chemical Physics of RAS, Chernogolovka, Moscow Region, Russia [c] Physics Division, School of Technology, Aristotle University of Thessaloniki, Thessaloniki, Greece [d] Department of Applied Sciences, Technological Educational Institute of Thessaloniki, Sindos, Greece

PLEASE SCROLL DOWN FOR ARTICLE

Taylor & Francis
Taylor & Francis Group

Thermally Induced Softening of the Radial Breathing Modes of Bundled Single-Walled Carbon Nanotubes

K. P. MELETOV[1], A. V. KRESTININ[2], J. ARVANITIDIS[3,4], D. CHRISTOFILOS[3] AND G. A. KOUROUKLIS[3]

[1]Institute of Solid State Physics of RAS, Chernogolovka, Moscow Region, Russia
[2]Institute of Problems of Chemical Physics of RAS, Chernogolovka, Moscow Region, Russia
[3]Physics Division, School of Technology, Aristotle University of Thessaloniki, Thessaloniki, Greece
[4]Department of Applied Sciences, Technological Educational Institute of Thessaloniki, Sindos, Greece

Raman spectra of purified arc-discharge single-walled carbon nanotubes (SWCNTs) were measured at temperatures up to 750 K. The temperature-induced frequency shift is reversible for the tangential G modes and irreversible for the radial breathing modes (RBMs). The residual softening of the RBMs increases with the tube diameter, whereas its dependence on the treatment temperature exhibits a threshold-like character. The mode softening can be attributed to removal of adsorbents and/or destruction of random C−C bonds between adjacent nanotubes caused by the high temperature treatment (HTT).

Keywords Raman spectra, Single-walled carbon nanotubes

Introduction

The temperature dependence of the nanotube diameter and the expansion of the bundle lattice due to anharmonicity of the van der Waals interaction were studied by X-ray diffraction (1). The thermal expansion coefficient for the tube diameter is very small, while the expansion coefficient of the bundle lattice is larger than that of graphite in the *c*-axis direction (1). Another X-ray diffraction study revealed the important role of adsorbents in the temperature behavior of bundled SWCNTs (2). The temperature dependence of the lattice constant of purified SWCNTs differs for the first heating and cooling cycles, indicating the shrinkage of the SWCNT bundles. The second and subsequent temperature runs show temperature dependence similar to that of the first cooling cycle, while exposure of the samples in the atmosphere leads to the recovery of the initial temperature dependence. The shrinkage of the SWCNT bundles under heating was attributed to removal of adsorbents, which are present in the interstitial channel sites or inside the nanotubes due to the high adsorption ability of bundled SWCNTs of atmospheric N_2 and O_2 gases (3). In addition, the temperature shift of the RBM and the G mode frequencies in bundled single- and double-walled carbon nanotubes was studied by Raman spectroscopy at temperatures up to 800 K (4,5). The Raman study and molecular dynamics simulations of bundled HiPCO SWCNT

has shown important contributions of the intratubular bond softening and the softening of the van der Waals intertubular interaction in the temperature shift of the RBM and the G band (4). Molecular dynamics simulations show small radial expansion of nanotubes, which does not contribute much in the temperature shift of the Raman peaks (4). This result is consistent with the X-ray diffraction study, which suggests even negative temperature expansion of the tube diameter (1).

The important feature of SWCNTs is their ability to aggregate in bundles. The isolation of individual nanotubes is possible only by ultrasonic exfoliation of bundles in water-surfactant dispersions (6). The aggregation is due to high cohesive energy of the van der Waals interaction, which is a few times higher than that of the C_{60} fullerene molecules for equivalent tube length (7). Taking into account the long length of nanotubes, their interaction becomes very strong, resulting in the formation of a hexagonal lattice of aligned closed packed nanotubes. Another reason for strong bonding may be the interlinking via C—C intertubular bonds due to a large number of unsaturated double C=C bonds similar to polymerized C_{60} fullerene. The illumination of C_{60} by light results in covalent bonding between adjacent C_{60} molecules and the creation of fullerene dimers and oligomers, while the high pressure/high temperature treatment of C_{60} results in the formation of bulk crystalline polymers (8–10). The interlinking of nanotubes assumes their deformation in radial direction requiring high pressure (11). Numerical calculations predict one- and two-dimensional networks of interlinked SWCNTs, some of which are energetically more stable than the hexagonal lattice formed via the van der Waals interaction (11). The SWCNT bundles under high pressure/high temperature treatment show irreversible changes in their structure and Raman spectra that provide evidence for covalent interlinking through sp^3 C—C bonds (12). The random interlinking of nanotubes caused by light illumination at ambient conditions similar to the photopolymerization of C_{60} cannot be excluded. On the other hand, the treatment of the fullerene polymers at temperatures higher than ~550 K results in the destruction of intermolecular C—C bonds and recovering of the initial *fcc* structure (13). Similarly, the HTT of bundled SWCNT may result in the destruction of random C—C bonds, if interlinking really takes place. In view of this, we investigated the Raman spectra of purified bundled SWCNTs at temperatures up to 750 K. We find that the temperature shift of the RBM frequencies is partially irreversible, resulting in a residual softening of the RBMs. The softening is larger for large tube diameters, whereas its dependence on the treatment temperature has a threshold-like character.

Experimental Details

The starting SWCNT material was synthesized by the arc discharge evaporation method in helium atmosphere at a pressure of 0.86 bar using a metallic Ni/Y catalyst. A purification method based on the multistep oxidation in air and reflux in HCl resulted in a ~90wt% content of SWCNTs. No surfactants were applied during the purification procedure. The main impurities were graphite particles in the order of 2–4 μm, while the total content of metal impurities was ~1.3%. The final material was a black fluffy powder that consisted of ~100 μm nanotube mats (14). The purified SWCNTs were annealed in vacuum at 873 K for 5 hours. The average diameter of the nanotubes was 1.5 nm, as it follows from the preparation method, the transmission electron microscopy, and Raman characterization. Raman spectra from small SWCNT samples were recorded *in-situ* in the back-scattering geometry using a micro-Raman setup comprised of a triple monochromator (DILOR XY) and a CCD detector system, cooled at liquid nitrogen temperature. The 514.5 nm Ar$^+$ laser line was focused on the sample by means of a 20× objective in a spot of ~3 μm diameter,

while the beam intensity on the sample was ∼1 mW. For the high temperature measurements, a home-made high temperature cell with temperature controller that maintained temperatures up to 750 K with an accuracy ±2 K was used.

Results and Discussion

The Raman spectrum of the purified SWCNTs recorded at ambient conditions in the regions of the RBM and the G modes is shown in Figure 1a. The G band corresponds to the tangential C−C stretching vibrations of SWCNTs that splits to the G$^-$ (circumferential component for a semiconducting nanotube) and to the G$^+$ (axial component for a semiconducting nanotube) bands, located at 1568 cm^{-1} and 1591 cm^{-1}, respectively. The RBM band is composed of a prominent peak at 170 cm^{-1}, and shoulders at ∼179 cm^{-1} and ∼160 cm^{-1}. The RBM frequency, ω_R, is inversely proportional to the tube diameter, d_t, while its value is upshifted due to the intertube interaction within a SWCNT bundle, as it follows from one of the empirical relations (15):

$$d_t(nm) = \left[234\,nm \cdot cm^{-1}\right] / \left[\omega_R\left(cm^{-1}\right) - 12\,cm^{-1}\right] \tag{1}$$

According to equation (1), the main RBM peak at 170 cm^{-1} corresponds to a SWCNT with a diameter of ∼1.48 nm, whereas the shoulders at 160 and 179 cm^{-1} correspond to SWCNTs with diameters ∼1.58 nm and ∼1.4 nm, respectively. Figures 1b and 1c show the Raman spectra after high temperature treatment of the SWCNTs at 530 K and 630 K, respectively. The RBMs soften after HTT; the softening is larger for large tube diameters and higher treatment temperatures, resulting in better separation of bands. The HTT does not affect the G modes within the accuracy of the measurements.
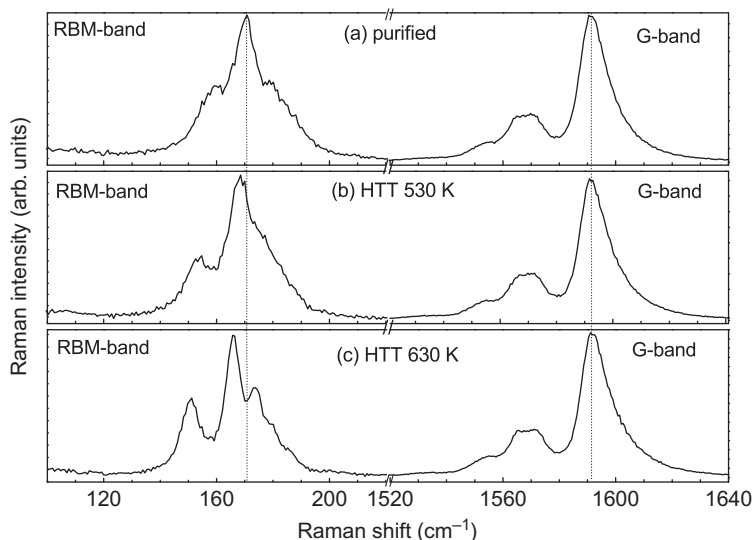
Figure 1. Raman spectra in the RBM and the G band frequency regions of **(a)** purified SWCNTs, **(b)** SWCNTs after HTT at 530 K, and **(c)** SWCNTs after HTT at 630 K. All spectra are recorded at the same sample site and at ambient conditions.

The temperature dependence of the RBM and the G mode frequencies, obtained from Raman spectra of the purified SWCNTs in three temperature runs, are shown in Figure 2. The open (solid) symbols denote the results of the heating (cooling) temperature cycle. The Raman spectra of the heating cycle were measured with a step of 25 K. The increase of temperature, its stabilization at the new value and the accumulation of Raman signal takes about 1 hour. The cooling cycle performed with a step of 50 K lasts longer due to the relatively large mass and thermal inertia of the heater. The circles in Figure 2 clearly show the irreversible temperature dependence of the RBM frequencies, which results in a residual softening of the modes during the first temperature run in the region 300–430 K. Squares in Figure 2 show the temperature dependence of the RBM frequencies obtained during the second temperature run performed in the region 455–530 K. The Raman spectra, recorded at the same sample site, show again an irreversible temperature dependence of the RBM frequencies and further residual softening of modes. The residual softening of the RBMs depends on the tube diameters; its value decreases with the decrease of the tube diameter and for the smallest ones becomes zero within the experimental accuracy. The third temperature run, performed in the temperature region 300–730 K, is reversible (triangles in Figure 2). The temperature dependence of the G mode frequencies obtained during the same temperature runs is also shown in Figure 2 and is reversible within the experimental accuracy.

The residual softening of the RBMs under various HTT conditions was studied in a number of independent temperature runs. The magnitude of the residual softening was
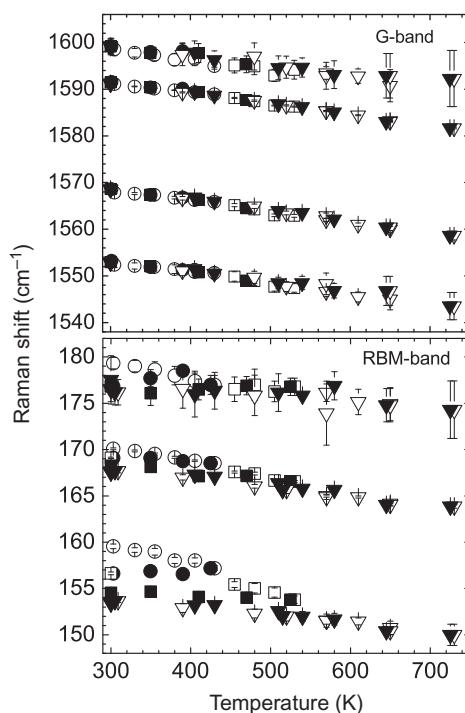
Figure 2. Temperature dependence of the RBM and the G mode Raman frequencies of the purified SWCNTs. The open (solid) symbols denote the heating (cooling) cycle. Circles: first temperature run (300–430 K), squares: second temperature run (300–530 K), triangles: third temperature run (300–730 K).
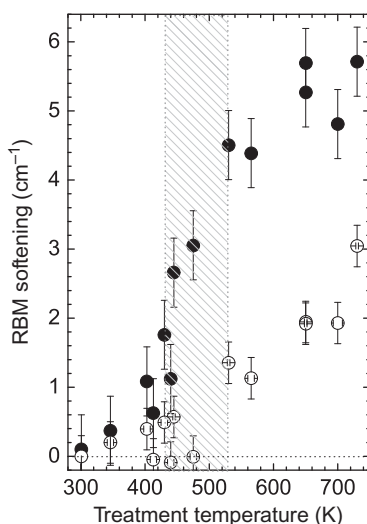
Figure 3. The dependence of the RBM residual softening on the treatment temperature. Open circles: SWCNTs with diameters ~1.48 nm, solid circles: SWCNTs with diameters ~1.58 nm.

determined as the difference of the RBM frequencies of the room temperature Raman spectra measured before and after sample treatment at temperatures up to 750 K for ~30 minutes. Spectra were recorded at the same site of the sample, and a new sample was used in each temperature run. The dependence of the RBM residual softening on the treatment temperature is illustrated in Figure 3. The open and solid circles correspond to the softening of the RBM related to tube diameters 1.48 nm and 1.58 nm, respectively. The softening of the modes is rather small for treatment temperatures up to ~430 K. At higher temperatures, the softening rapidly increases to almost its maximum value above ~530 K. Further increase of the treatment temperature does not result in a significant increase of the RBM residual softening.

The most interesting effect in the temperature behavior of the Raman spectra of bundled SWCNT is this threshold-like dependence of the RBM softening with a threshold temperature in the range 430–530 K. The softening of the RBMs should be related to the irreversible increase of the tube diameter and/or decrease of the intertube interaction near the threshold temperature. According to molecular dynamics calculations, the influence of the intertube van der Waals interaction on the vibrational spectrum of bundled SWCNT was found to diminish with increasing phonon frequency, and the effect of interaction is negligible at phonon frequencies higher than 500 cm^{-1} (16). Consequently, the influence of the intertube interaction potential on the G mode frequency is negligible, explaining its reversible temperature dependence irrespectively from any changes in the interaction potential. On the contrary, the influence of the intertube interaction on the low frequency vibrations is strong and may result in an irreversible softening of the RBMs when the interaction is decreased. In addition, the influence increases with the decrease of the RBM frequency resulting in larger softening of the low frequency RBMs (16).

To clarify the nature of the irreversible temperature effects in bundled SWCNT, we have to analyze various effects that may cause irreversible changes in the intertube interaction and/or in the tube diameters after HTT. Regarding to the tube diameter, its thermal expansion coefficient is almost zero, so the tube diameter remains practically unchanged under sample

heating (1). The irreversible increase of the tube diameter is possible due to coalescence of nanotubes observed after HTT at ~1800 K in H_2 atmosphere, resulting in diameter-doubled nanotubes (17). Obviously, this is not our case because of the different temperature conditions and the considerably larger mode softening anticipated due to the doubling of the nanotube diameter.

The irreversible changes in the intertube interaction under HTT may be caused by removal of adsorbed atmospheric N_2 and O_2 gases, which may be present in the interstitial channel sites or inside the nanotubes due to the high adsorption ability of bundled SWCNT (3). The bundle lattice constant of the purified SWCNTs decreases irreversibly from 17.1 to 16.9 Å in the first heating/cooling run due to desorption of molecules from the intertube space of SWCNTs heated under vacuum (2). The radial shrinkage of SWCNT bundles takes place in the temperature region 300–600 K. The decrease of the bundle lattice constant should result in the increase of the intertube interaction and the upshift of the RBM frequencies in contrast to our experimental observations. One may assume that the presence of adsorbed molecules in the interstitial channel sites of bundles results in the enhancement of the intertube interaction and thus their removal will decrease the overall interaction despite the intertube distance shortening. Unfortunately, there are no computer simulation data related to the influence of adsorbents on the van der Waals interaction in bundled SWCNT for a quantitative estimation of this possibility.

The irreversible increase of the intertube distance may be caused by destruction of random C−C bonds between the nanotubes under HTT of bundled SWCNTs. The random interlinking of nanotubes that might take place under light illumination at ambient conditions assumes a decrease of the mean intertube distance and local deformation of the nanotubes in the radial direction near the link. The HTT of bundled SWCNTs may result in the destruction of C−C intertube bonds similar to the case of HTT of crystalline polymers of C_{60} (13). Then, the threshold-like character of the RBM softening can be interpreted as an indication of such destruction.

Conclusions

The Raman data presented in this paper clearly show the irreversible changes in the intertube interaction of bundled SWCNT caused by their treatment at high temperature. The nature of these changes is not quite clear yet and additional investigations, like differential scanning calorimetry and time-dependent annealing experiments, will be required.

Acknowledgments

References

1. Maniwa, Y., Fujiwara, R., Kira, H., Hideki Tou, Kataura, H., Suzuki, S., Achiba, Y., Nishibori, E., Takata, M., Sakata, M., Fujiwara, A., and Suematsu, H. (2001) Thermal expansion of single-walled carbon nanotubes (SWNT) bundles: X-ray diffraction studies. *Phys. Rev. B*, 64: 241402-1–21402-3(R).
2. Yosida, Y. (2002) Radial shrinkage of single-walled carbon nanotube bundles at high temperature. *The Rigaku Journal*, 19: 42–46.

3. Fujiwara, A., Ishii, K., Suematsu, H., Kataura, H., Maniwa, Y., Suzuki, S., and Achiba, Y. (2001) Gas adsorption in the inside and outside of single-walled carbon nanotubes. *Chem. Phys. Lett.*, 336: 205–211.

4. Raravikar, N. R., Keblinski, P., Rao, A. M., Dresselhaus, M. S., Schadler, L. S., and Ajayan, P. M. (2002) Temperature dependence of radial breathing mode Raman frequency of single-walled carbon nanotubes. *Phys. Rev. B*, 66: 235424-1–235424-9.

5. Zhou, Z., Ci, L., Song, L., Yan, X., Liu, D., Yuan, H., Gao, Y., Wang, J., Liu, L., Zhou, W., Xie, S., Du, Y., and Mo, Y. (2004) The intrinsic temperature effect of Raman spectra of doubled-walled carbon nanotubes. *Chem. Phys. Lett.*, 396: 372–376.

6. O'Connell, M. J., Bashilo, S. M., Huffman, C. B., Moore, V. C., Strano, M. S., Haroz, E. H., Rialon, K. L., Boul, P. J., Noon, W. H., Kittrell, C., Ma, J., Hauge, R. H., Weisman, R. B., and Smalley, R. E. (2002) Band gap fluorescence from individual single-walled carbon nanotubes. *Science*, 297: 593–596.

7. Girifalco, L. A., Hodak, M., and Lee, R. S. (2000) Carbon nanotubes, buckyballs, ropes, and a universal graphitic potential. *Phys. Rev. B*, 62: 13104–13110.

8. Rao, A. M., Zhou, P., Wang, K.-A., Hager, G.T., Holden, J. M., Wang, Y., Lee, W.-T., Bi, X.-X., Eklund, P. C., Cornett, D. S., Duncan, M. A., and Amster, I. J. (1993) Photoinduced polymerization of solid C_{60} films. *Science*, 259: 955–957.

9. Iwasa, Y., Arima, T., Fleming, R. M., Siegrist, T., Zhou, O., Haddon, R. C., Rothberg, L. J., Lyons, K. B., Carter, Jr., H. L., Hebard, A. F., Tycko, R., Dabbagh, G., Krajewski, J. J., Thomas, G. A., and Yagi, T. (1994) New phases of C_{60} synthesized at high pressure. *Science*, 264: 1570–1572.

10. Nunez-Regueiro, M., Marques, L., Hodeau, J.-L., Bethoux, O., and Perroux, M. (1995) Polymerized fullerite structures. *Phys. Rev. Letters*, 74: 278–281.

11. Yldirim, T., Gülseren, O., Kiliç, Ç., and Ciraci, S. (2000) Pressure-induced interlinking of carbon nanotubes. *Phys. Rev. B*, 62: 12648–12651.

12. Khabashesku, V. N., Gu, Z., Zimmerman, J. L., Margrave, J. L., Davydov, V. A., Kashevarova, L. S., and Rakhmanina, A. V. (2002) Polymerization of single-walled carbon nanotubes under high pressures and high temperatures. *J. Phys. Chem.*, 106: 11155–11162.

13. Iwasa, Y., Tanoue, K., Mitani, T., and Yagi, T. (1998) Energetics of polymerized fullerites. *Phys. Rev. B*, 58: 16374–16377.

14. Krestinin, A. V., Raevskii, A. V., Kiselev, N. A., Zvereva, G. I., Zhigalina, O. M., and Kolesova, O. I. (2003) Optical activity effect in crystalline structures of purified single-wall carbon nanotubes. *Chem. Phys. Lett.*, 381: 529–534.

15. Venkateswaran, U. D. (2004) Squeezing carbon nanotubes. *Phys. Stat. Sol. (b)*, 241: 3345–3351.

16. Dresselhaus, M. S. and Eklund, P. C. (2000) Phonons in carbon nanotubes. *Advances in Physics*, 49: 705–814.

17. Fang, S.L., Rao, A. M., Eklund, P. C., Nikolaev, P., Rinzler, A. G., and Smalley, R. E. (1998) Raman scattering study of coalesced single-walled carbon nanotubes. *Journal of Material Research*, 13: 2405–2411.